Long-wavelength multiphoton ionization inside band-gap solids

D. Grojo,[1,*] S. Leyder,[1] P. Delaporte,[1] W. Marine,[2] M. Sentis,[1] and O. Utéza[1]
[1]*Aix-Marseille University, CNRS (Centre National de la Recherche Scientifique), LP3 UMR7341, F-13288 Marseille, France*
[2]*Aix-Marseille University, CNRS (Centre National de la Recherche Scientifique), CINAM UMR7325, F-13288 Marseille, France*
(Received 20 August 2013; published 19 November 2013)

Using various band-gap materials and tightly focused femtosecond laser pulses with wavelengths in the range 1200–2200 nm, we show that nonlinear absorption is independent of the wavelength except for narrow gap semiconductor materials. This observation corresponds to a transition between multiphoton ionization and tunnel ionization for an adiabaticity parameter of about 3, which compares favorably with Keldysh predictions. Our results indicate that long wavelengths must open up an alternative to pulse shortening for ultraprecision optical breakdown in dielectrics.

DOI: 10.1103/PhysRevB.88.195135 PACS number(s): 79.20.Ws, 33.80.Wz, 78.20.−e, 79.20.Ds

Optical breakdown with tightly focused intense femtosecond laser pulses promotes various applications in dielectrics. These include ultra-high-resolution surface ablation,[1] waveguide writing,[2] and more generally the direct fabrication of three-dimensional (3D) devices inside materials.[3] In optical breakdown, the photoionization (PI) precedes the development of avalanche ionization and therefore acts as an initial step in the laser energy deposition and subsequent material modifications.[4] Although such modifications have been extensively studied, the PI physics remains only partially understood and controlled in the experiments.

Depending on the laser parameters, there are two different regimes of PI that are expected: the multiphoton ionization (MPI) regime and the tunneling ionization (TI) regime.[5] Here we will concentrate on a major difference between these processes: their wavelength dependence. This is shown in Fig. 1 with the results of numerical calculations for the PI rate as a function of intensity and wavelength using rigorously the formulation common for both processes proposed by Keldysh.[5] From the Keldysh theory, the adiabaticity parameter $\gamma = \omega\sqrt{m\Delta_{\mathrm{BG}}}/eE$ (where ω, m, E, and Δ_{BG} are, respectively, the laser frequency, the reduced mass of the electron-hole pair, the magnitude of the laser electric field, and the band gap of the material) can be used to position the transition from MPI to TI.

For all wavelengths considered here, the photon energy of the laser radiation is less than the band gap and so the energy of many photons has to be supplied simultaneously to promote an electron to the conduction band. This results in a strong dependence on the laser intensity and the wavelength for $\gamma \gg 1$, where the MPI picture holds. For $\gamma \ll 1$, the Keldysh theory coincides with a PI rate given by $W(I) \propto \exp[-2\Delta_{\mathrm{BG}}^{3/2}\sqrt{m}/(3e\hbar E)]$, very similar to the Zener formulation for atoms and molecules[6] except that the exponent is reduced by a factor of 2. Then, the ionization rate becomes dependent not just directly on the intensity but on the laser field strength because the ionization relies on the suppression of the binding potential near the peaks of the electric field at half-optical cycles of the pulse. A major consequence is that the wavelength dependence of the PI rate vanishes.

The TI regime is of major interest for fundamental considerations but also for laser microfabrication applications because it is usually associated with an increase of determinism for material breakdown. Then, the interaction becomes extremely reproducible, leading to increased precision laser machining capabilities.[1,7] There are two ways in which the adiabaticity parameter can be reduced in experiments. The first option is to increase the intensity, leading to energy deposition. Thus, there is a general trend to pulse shortening.[4,7,8] The second option relies on a change of the wavelength toward the near-infrared (NIR) and mid-infrared (MIR) part of the spectrum.

In this paper, we concentrate on this second option and we investigate the interaction of femtosecond lasers with wavelengths increased to the region 1200–2200 nm. By measuring the wavelength dependence of the nonlinear absorption, we gauge the photoionization mechanisms for various band-gap materials. Using tightly focused beams, we find the signature of the TI for all dielectrics and the increasing importance of MPI with the decrease of the band gap for semiconductor materials. Our results compare favorably with Keldysh's predictions. They illustrate opportunities and challenges in 3D laser micromachining in dielectrics and its extension to semiconductors.

For the interpretation of these highly nonlinear processes, we must be able to accurately estimate the laser intensity in the interaction volume for all tested wavelengths. We have carefully arranged the experiment so that all important parameters are controlled. A Ti:sapphire laser (Spectra-Physics, Hurricane) emitting linearly polarized 800-nm radiation pulses with a minimum duration of 100 fs and a repetition rate of up to 1 kHz is used as the master laser source. Longer wavelengths are produced by directing 500 μJ of the 800-nm radiation into an optical parametric amplifier (OPA) (Spectra-Physics, 800CF), which outputs up to 90 μJ (signal and idler). A dichroic filter is used to separate the signal from the idler. From this source, we select six wavelengths: 1200, 1300, 1400, 1580 (signal), 2000, and 2200 nm (idler). For each wavelength, the beam additionally propagates through a long pass interference filter. The pulse duration τ_{las} is 110 fs [full width at half maximum (FWHM)] at the OPA output as measured by a NIR single shot autocorrelator (Light Conversion, TiPA AT5C3). Spectral measurements of the pulses give a typical pulse bandwidth of $\approx$30 nm (FWHM at 1300 nm), slightly larger than that for transform limited pulses with the same duration (22 nm).

 ©2013 American Physical Society

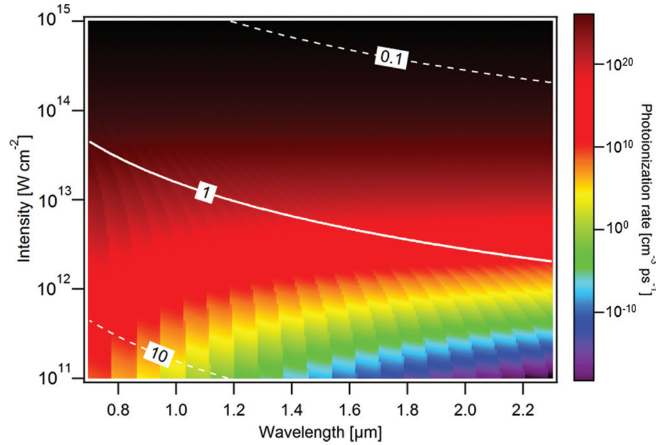

FIG. 1. (Color online) Calculated PI rate (logarithmic scale) in the intermediate regime as a function of wavelength and laser intensity according to the Keldysh formulation. The conditions corresponding to an adiabaticity parameter equal to 0.1, 1, and 10 are marked by contour lines. The calculation assumes a band gap of 9 eV (the a-SiO_2 case). The strong wavelength dependence associated with multiphoton ionization vanishes for $\gamma < 1$ (strong field and/or long wavelength).

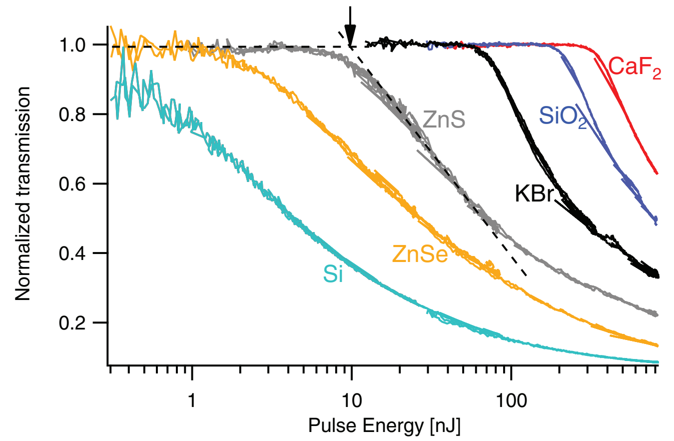

FIG. 2. (Color online) Measured transmission of tightly focused femtosecond laser pulses as a function of pulse energy for dielectrics and semiconductors with band-gap energies varying from 1.1 to 11.8 eV (see Table I). The dotted lines and the arrow illustrate the procedure which is used to extract the nonlinear absorption thresholds from the measurements (the ZnS case).

The laser pulses are focused into the materials at a depth of about 0.2 mm below the surface using a NIR microscope objective with a numerical aperture (NA) of 0.3 (Olympus, LMPLN10XIR). Most of the experiments are also repeated using a 0.53 NA reflective objective (Newport) to confirm that the measurements are not affected by chromatic or dispersion effects (not shown here). The tight focusing allows us to reach high intensities without the propagation's being influenced by self-focusing or self-phase modulation, as checked by measurements of the transmitted spectrum. These conditions ensure also in-the-bulk confined interactions while avoiding the effects associated with spherical aberrations.[9]

The studied materials are listed in Table I together with their known band gaps. We note that all these materials are transparent at the wavelengths considered. For silicon dioxide, we use a high-purity amorphous fused silica material (Suprasil I, Heraeus). All other substrates are high-purity optical grade crystals polished on both sides for transmission measurements (Edmund Optics). All substrates have a thickness >2 mm, which ensures that there is no interaction with the back surface during the experiments.

The transmission of the ionizing pulses T is measured by using integrating spheres equipped with Ge (signal) or cooled InGaAs photodetectors (idler) in a reference arm and a transmitted signal arm. The combination of two broadband NIR nanoparticle linear polarizers enables variable attenuation of the incident beams. The materials are placed on a translation stage and the photodetectors are connected to an automated acquisition system to perform the measurements as a function of the incident pulse energy, with each shot interacting with fresh material.

TABLE I. Band-gap materials used in the experiments.

	Material	Band gap Δ_{BG} (eV)
Calcium fluoride	CaF_2	11.8 (direct)
Silicon dioxide	a-SiO_2	9 (direct)
Potassium bromide	KBr	7.6 (direct)
Zinc sulfide	ZnS	3.6 (direct)
Zinc Selenium	ZnSe	2.7 (direct)
Silicon	Si	1.1 (indirect)

Figure 2 shows the transmission data at 1300 nm as a function of the incident pulse energy for all tested materials. The curves are normalized to the low-intensity transmission T_0 accounting for Fresnel boundary reflection losses. At low laser-pulse energies, all curves (T/T_0) exhibit 100% transmission except for silicon, which has a threshold below the sensitivity limit of our diagnostics (≈1 nJ). When the laser energy reaches a level above which nonlinear absorption is initiated, a strong decrease of the transmission is observed. As expected, the energy threshold for nonlinear absorption decreases markedly with the nonlinear order of the interactions.

Multiphoton absorption is not the only process which attenuates the beam, because it also injects electron-hole pairs, leading to free-carrier absorption, avalanche, and plasma effects at large excitation densities. The saturation of the transmission curves at high pulse energies is attributed to plasma defocusing and screening effects,[10,11] which are beyond the scope of the present paper. From here on we will concentrate on the early portions of the transmission curves, to neglect these effects and focus on the PI physics.

With tight focusing in the bulk of materials, we expect nonlinear absorption to arise in the so-called intermediate PI regime ($0.1 < \gamma < 10$) where the TI process may contribute. To confirm this aspect, we compare the intensity dependence of the nonlinear absorption to a theoretical multiphoton power law $\propto I^N$ for each material. Figure 3 shows the absorption measurements as a function of laser intensities close to the threshold (note the logarithmic scales). The absorption is retrieved from the measurements by simply assuming $A = 1 - T/T_0$. Of course, to plot the intensity response we must take into account differing focal spot diameters while varying the laser wavelength. Before the experiments, the

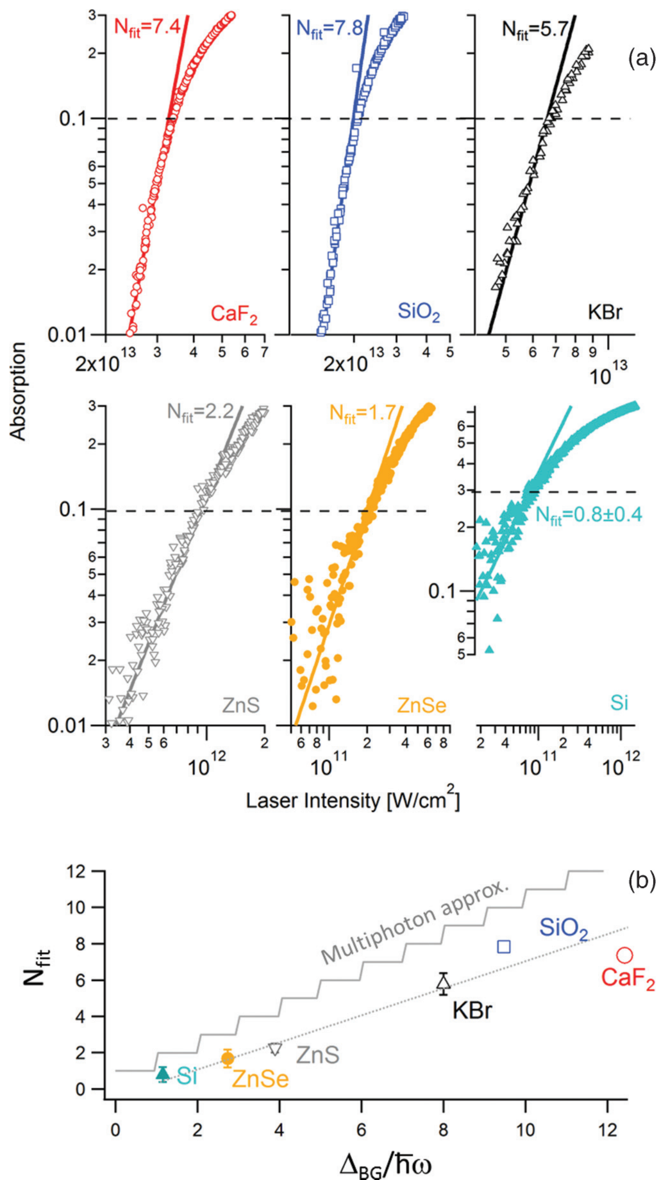

FIG. 3. (Color online) (a) Measurements of nonlinear absorption at 1300-nm wavelength when focusing 110-fs laser pulses with a 0.3 NA microscope objective. The solid lines show the comparison with a scaling law I^N, where N is the fitting parameter. (b) Comparison between N found with the fitting procedure (N_{fit}) and theoretical values for a multiphoton approximation (solid line). For all tested cases, we note that $N_{\text{fit}} < N_{\text{theo}}$.

beam was analyzed using the residual response of a silicon CCD analyzer at 1300-nm wavelength (Gentec, CCD23-1310). At the optimum operation of the OPA, we could deliver a beam with a measured M^2 factor equal to 1.07 (beam caustic measurement). The good Gaussian beam profile allows us to estimate the focal spot size to be $2\omega_0 = 1.22\lambda/\text{NA}$ in the experiments (5.3 μm at 1300 nm and 8.9 μm at 2200 nm).

In Fig. 3(a), we note that we can describe the growth of the nonlinear losses at low intensities ($A < 0.1$) using a power law for all tested materials. For silicon, due to the limitations of our measurements (sensitivity), the fitting procedure requires taking into account higher absorption measurements ($A < 0.3$, horizontal dashed line). This leads to a rather imprecise evaluation. Nevertheless, if losses resulted only from multiphoton absorption, the slope (N_{fit} parameter) should correspond to the theoretical value $N_{\text{theo}} = \lceil \Delta_{\text{BG}}/\hbar\omega \rceil$ where $\lceil . \rceil$ denotes the ceiling function. Also, one would expect an increase of the apparent slope ($N > N_{\text{theo}}$) if avalanche ionization were to assist the MPI with an exponential growth of the free-carrier density.[12] However, Fig. 3(b) shows that we find N_{fit} systematically below N_{theo}. This lower laser intensity dependence is compatible with a significant TI contribution (see Fig. 1; $\gamma < 1$), confirming in this way the intermediate PI regime.

As we mentioned, measuring the wavelength dependence of the ionization thresholds is another useful approach to evaluating the relative importance of the two PI channels in the initiation of nonlinear absorption. We performed transmission measurements similar to those shown in Fig. 2 with all available wavelengths but concentrating on two very different materials: Si and a-SiO_2. We chose to investigate the bulk response of these two materials because of their technological importance but also because their nonlinear absorption thresholds are obtained for significantly different adiabaticity parameters. According to the measurement at 1300 nm (Fig. 2), we will see that we reach $\gamma = 9.2$ in Si while it is below unity for SiO_2.

From all the measurements, the threshold for nonlinear absorption is determined carefully by the method of a two-segment fit: the point at which the straight line of 100% transmission (horizontal) intersects the straight line fit of absorption above the threshold. An example of this threshold extraction procedure is shown in Fig. 2 for the ZnS case (see dashed lines and arrow).

Figure 4 shows the intensity thresholds measured as a function of the laser wavelength. Interestingly, we note that the intensity threshold for nonlinear absorption is independent of the wavelength in a-SiO_2, whereas the multiphoton order varies from 9 to 16 for the tested wavelengths. We measured that the nonlinear absorption is initiated for an intensity threshold of $\approx 2 \times 10^{13}$ W cm^{-2}, slightly higher than that found at 800 nm under very similar conditions.[12,13] We obtain different bulk responses for silicon when we change the wavelength. Between 1300 and 2000 nm, the photon energy puts us in a low-order two-photon absorption regime and we find modest variations for the threshold. At 1200 nm, the lower threshold value is attributed to residual linear absorption. For $\lambda > 1900$ nm, a significant increase of the threshold corresponds to the transition from the two- to the three-photon absorption regime. The positions of the transitions are in good agreement with recent multiphoton absorption cross-section measurements using loosely focused beams in the same wavelength range.[14,15] According to these results, the wavelength dependence as a signature of the relative importance of MPI with respect to TI (see Fig. 1) compares favorably with the response of these two materials.

To study in more detail the response as a function of γ, we investigate the response of all our materials (see Table I). Then, γ is varied gradually through the ratio $\Delta_{\text{BG}}/I_{\text{th}}$ because obviously I_{th} does not scale linearly with the band gap due to the nonlinear nature of the interactions. To quantify the

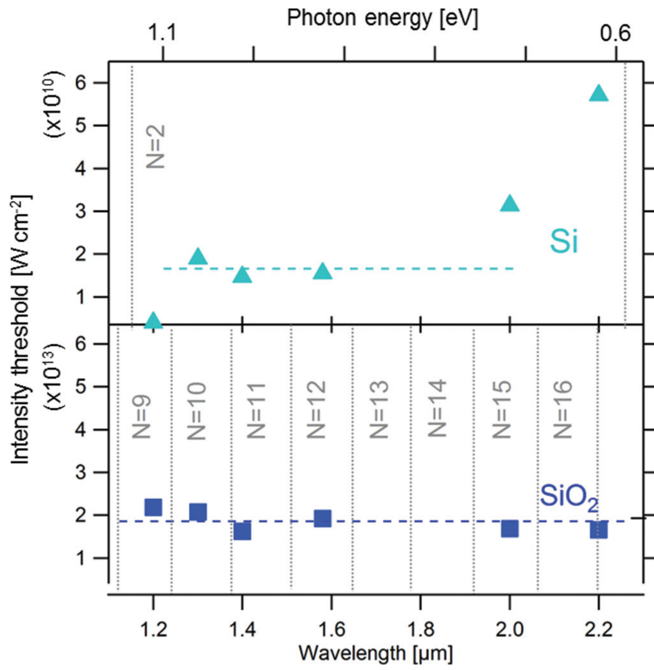

FIG. 4. (Color online) Wavelength dependence of nonlinear absorption thresholds for a-SiO_2 and Si for the same laser sources at different wavelengths focused with a 0.3 NA NIR microscope objective. The domains associated with each theoretical multiphoton order $N = \lceil \Delta_{BG}/\hbar\omega \rceil$ are also displayed in the graphs (gray vertical lines).

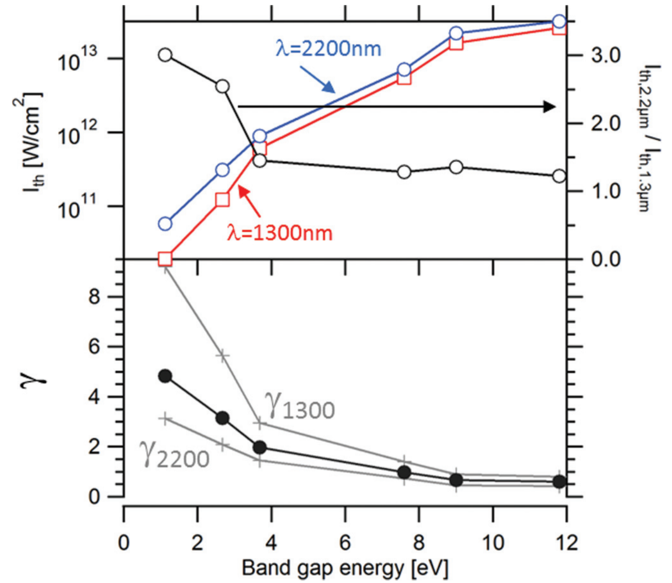

FIG. 5. (Color online) Comparison between intensity thresholds for nonlinear absorption at 1300- and 2200-nm wavelengths as a function of band-gap value for all tested materials. The right axis (top graph) shows the ratio between both thresholds. The lower graph displays the values of the adiabaticity parameter corresponding to the measured thresholds for both wavelengths. The intensity threshold for nonlinear ionization at 2200 nm deviates from the threshold at 1300 nm only for the smallest gap values (ZnSe, Si) where the situations lead to $\gamma > 3$.

dependence of the nonlinear absorption intensity threshold on the wavelength, for all the materials, we chose two well-separated wavelengths: 1300 and 2200 nm. We avoid 1200 nm because residual linear absorption was found for Si (see Fig. 4). Figure 5 shows the results of this measurement as a function of the band-gap value for the materials. For ease of comparison, we also show the ratio between the two thresholds for all materials (right axis). We note that both wavelengths lead to very similar thresholds for all materials tested except for ZnSe and Si, corresponding to the interactions with the lowest multiphoton orders. The bottom graph of Fig. 5 displays the corresponding γ values for all threshold measurements. Because γ depends on the wavelength, we calculated for each material an averaged γ using $\lambda = 1750$ nm and $I = (I_{\text{th, 2.2}\,\mu\text{m}} + I_{\text{th, 1.3}\,\mu\text{m}})/2$ (black curve). We note that γ increases gradually when decreasing the band gap, and we can conclude that the wavelength dependence arises for a typical γ value exceeding 3. Here, it is worth noting that Si is an indirect band-gap semiconductor (see Table I), which implies the involvement of phonons for the ionization events. It is likely that the band structure plays a role in the measured responses. However, since we found a wavelength dependence for Si but also for ZnSe, which is a direct band-gap material, we can conclude that the γ-based dichotomy for the mechanisms remains robust to these considerations for the materials of this study.

In summary, there had been no direct experimental evidence of tunneling dynamics inside solids until recently.[16,17] We have shown that the wavelength independence of nonlinear absorption represents a direct experimental observable for the importance of TI. Using long wavelengths in a typical configuration for femtosecond laser micromachining, we found the signature of TI for all dielectrics at the initiation of energy deposition while the MPI response persists for narrow gap materials. We have concentrated on long wavelengths in the range 1200–2200 nm. This was a convenience but not a limitation. The wavelength of femtosecond lasers can be pushed to the MIR part of the spectrum[18] with OPA systems to even further enhance the importance of TI in these situations.

Today, there is a general trend toward the production of extremely short pulses to decrease γ and to reach deterministic breakdown regimes for advanced applications.[1,3] However, it is worth noting that the adiabaticity parameter varies implicitly as $\sqrt{\tau_{\text{las}}}$ whereas it varies as $1/\lambda$ when the wavelength is varied. Our results confirm that wavelength tuning toward the IR is an efficient alternative to pulse shortening. With our 110-fs laser pulses at 2200 nm, we already reach a γ value down to 0.45 at intensities required for energy deposition, which is similar to what is obtained with few optical cycle pulses at 800 nm for intensities leading to surface ablation.[7] In this perspective, long wavelengths open an interesting route but they provide also another advantage. They are desirable for the envisioned 3D applications in biological samples and in narrow gap semiconductors which are opaque at the fundamental wavelength of Ti:sapphire femtosecond lasers.

This research was funded by the French National Research Agency (ANR 2010-JCJC-913-01).

*grojo@lp3.univ-mrs.fr

[1] A. P. Joglekar, H. Liu, E. Meyhofer, G. Mourou, and A. J. Hunt, Proc. Natl. Acad. Sci. USA **101**, 5856 (2004).
[2] K. M. Davis, K. Miura, N. Sugimoto, and K. Hirao, Opt. Lett. **21**, 1729 (1996).
[3] R. R. Gattass and E. Mazur, Nature Photon. **2**, 219 (2008).
[4] M. Lenzner, J. Kruger, S. Sartania, Z. Cheng, C. Spielmann, G. Mourou, W. Kautek, and F. Krausz, Phys. Rev. Lett. **80**, 4076 (1998).
[5] L. Keldysh, Sov. Phys. JETP **20**, 1307 (1965).
[6] C. Zener, Proc. R. Soc. A **145**, 523 (1934).
[7] N. Sanner, O. Uteza, B. Chimier, M. Sentis, P. Lassonde, F. Legare, and J. C. Kieffer, Appl. Phys. Lett. **96**, 071111 (2010).
[8] A. P. Joglekar, H. Liu, G. J. Spooner, E. Meyhofer, G. Mourou, and A. J. Hunt, Appl. Phys. B **77**, 25 (2003).
[9] S. Leyder, D. Grojo, P. Delaporte, W. Marine, M. Sentis, and O. Uteza, Appl. Surf. Sci. **278**, 13 (2013).
[10] D. von der Linde and H. Schuler, J. Opt. Soc. Am. B **13**, 216 (1996).
[11] L. Sudrie, A. Couairon, M. Franco, B. Lamouroux, B. Prade, S. Tzortzakis, and A. Mysyrowicz, Phys. Rev. Lett. **89**, 186601 (2002).
[12] P. P. Rajeev, M. Gertsvolf, E. Simova, C. Hnatovsky, R. S. Taylor, V. R. Bhardwaj, D. M. Rayner, and P. B. Corkum, Phys. Rev. Lett. **97**, 253001 (2006).
[13] P. P. Rajeev, M. Gertsvolf, P. B. Corkum, and D. M. Rayner, Phys. Rev. Lett. **102**, 083001 (2009).
[14] A. D. Bristow, N. Rotenberg, and H. M. van Driel, Appl. Phys. Lett. **90**, 191104 (2007).
[15] S. Pearl, N. Rotenberg, and H. M. van Driel, Appl. Phys. Lett. **93**, 131102 (2008).
[16] M. Gertsvolf, M. Spanner, D. M. Rayner, and P. B. Corkum, J. Phys. B **43**, 131002 (2010).
[17] A. V. Mitrofanov, A. J. Verhoef, E. E. Serebryannikov, J. Lumeau, L. Glebov, A. M. Zheltikov, and A. Baltuska, Phys. Rev. Lett. **106**, 147401 (2011).
[18] D. M. Simanovskii, H. A. Schwettman, H. Lee, and A. J. Welch, Phys. Rev. Lett. **91**, 107601 (2003).